G. Consolati, D. Nichetti, F. Briatico Vangosa, F. Quasso
Beyond the Spherical Approximation: Elongated Free Volume Holes in Rubbers: a Positron Annihilation Study
Rubber Chemistry and Technology, Vol. 92, N. 4, 2019, p. 709-721
doi:10.5254/rct.19.80452

BEYOND THE SPHERICAL APPROXIMATION: ELONGATED FREE VOLUME HOLES IN RUBBERS: A POSITRON ANNIHILATION STUDY

GIOVANNI CONSOLATI,[1,2,*] DARIO NICHETTI,[3] FRANCESCO BRIATICO VANGOSA,[4] FIORENZA QUASSO,[1]

[1]DEPARTMENT OF AEROSPACE SCIENCE AND TECHNOLOGY, POLITECNICO DI MILANO, VIA LAMASA, 34, 20156 MILANO, ITALY

[2]INFN, SEZIONE DI MILANO, VIA CELORIA, 16, 20133 MILANO, ITALY

[3]RHEONIC LAB, VIA QUADELLE 2C, 26012 CASTELLEONE , ITALY

[4]DIPARTIMENTO DI CHIMICA, MATERIALI E INGEGNERIA CHIMICA "GIULIO NATTA," POLITECNICO DI MILANO, PIAZZA LEONARDO DA VINCI, 32, 20133 MILANO, ITALY

ABSTRACT

The free volume fraction, a key parameter for the understanding of mechanical and transport properties of polymers, has been evaluated in a fluoroelastomer and a *cis*-polyisoprene rubber by means of positron annihilation lifetime spectroscopy and dilatometry. The evaluation showed that the assumption of elongated holes allows one to get a very good agreement between the free volume fraction experimentally determined and the theoretical expectation based on the lattice-hole model. On the other hand, systematic discrepancies are found using the spherical approximation. Moreover, the average hole size is found to be correlated to the effective bond length l_{eff}, a parameter connected to reptation motions and largely independent of the polymer structure. The result sheds some light on conformational statistics for the most flexible linear polymers that approach Gaussian chain behavior. [doi:10.5254/rct.19.80452]

INTRODUCTION

Positron annihilation lifetime spectroscopy (PALS)[1] is one of the few experimental techniques able to supply information on the free volume, an important concept in designing polymers with desired performance. Indeed, relevant characteristics of polymers, such as mechanical and thermal properties,[2] as well as permeability,[3] are related to the free volume.[4] In addition, the size and the shape of the holes forming the free volume may play a role, for example, in gas separation membranes. PALS has the advantage of being non-destructive and does not use large probes, such as photochromic and fluorescent molecules,[5] which could influence the estimation of the free volume. PALS uses positronium, Ps, a bound state formed when a positron injected in the medium meets an electron of the surroundings. Ps mainly localizes in the voids of the material. Ground state Ps (the only one of interest in polymer research) exists in two sublevels, according to the different spin orientations of the two particles: para-Ps (*p*-Ps, antiparallel spins) and ortho-Ps (*o*-Ps, parallel spins).[6] Since the positron and electron are antiparticles, they annihilate, which makes Ps a valuable tool to study free volume holes, provided that its lifetime is shorter than that of the host cavity.

In vacuo, *p*-Ps self-annihilation occurs with emission of two γ rays; its lifetime is 125 ps. On the other hand, *o*-Ps has a lifespan of 142 ns, and three γ rays are emitted in the self-annihilation process. In a cavity, in addition to the intrinsic annihilation, *o*-Ps undergoes the "pickoff" process, consisting of the annihilation in two photons with an electron of the surroundings in a singlet spin state. This shortens the lifetime of *o*-Ps with respect to its value in vacuo, more so when the dimension of the hole is smaller. *p*-Ps is generally not considered in research on the free volume since its lifetime is scarcely influenced on passing from vacuum to matter.

Information on the specific free volume V_f

$$V_f = Nv_h \tag{1}$$

*Corresponding author. Email: giovanni.consolati@polimi.it

can be obtained from the knowledge of both v_h, the average hole volume, and N, the number density of holes. A comparison between specific volume and hole volume data, as obtained in the same conditions, supplies N.[7] Behavior of the specific volume versus temperature can be obtained by dilatometry. In particular, a pressure volume temperature (PVT)[8] machine is able to supply the variations of the specific volume in a range of temperatures, for pressures ranging from 20 to 200 MPa. Values at ambient pressure are obtained by extrapolation.

The variable v_h is known once the *o*-Ps lifetime is translated into a hole size, which requires the choice of a hole shape. The simplest approximation is the spherical one.[9,10] However, the calculation of the sizes of the holes, when framed into alternative geometries, produces different results—and therefore different free volume fractions—for a given *o*-Ps lifetime.[11] Any geometry framing the hole cannot be an exact description of it, since real holes are irregular. Nevertheless, it is important to distinguish, among the various approximate geometries, the most suitable one to get insight about the morphology for the holes of a given polymeric structure.

In the present work we compared the free volume fraction resulting from PALS and specific volume measurements with the theoretical fraction resulting from the Simha–Somcynsky lattice-hole theory.[12] This theory describes an amorphous assembly of chain molecules on a lattice with sites occupied by chain segments. In addition, to simulate molecular disorder, a fraction of vacancies is considered, which is a free volume quantity. The equation of state (see Eq. 5a below) derived from the theory relates specific volume and temperature of the polymer under investigation. The requirement of equilibrium (minimization of the Helmoltz free energy) produces a second relationship (Eq. 5b) between the two thermodynamic quantities, which allows the extraction of the free volume fraction by suitably fitting the specific volume data in a given range of temperatures. The equation has provided very good fits for more than 50 polymers and copolymers at equilibrium, that is, above the glass transition temperature, T_g.[13]

We investigated two different types of elastomers: a *cis*-polyisoprene rubber (IR) and a fluoro rubber (Fluor Kautschuck Mischung; FKM). Rubber has already been the subject of much PALS research.[14–17] In particular, Srithawatpong et al.[7] investigated the free volume in *cis*-polyisoprene using PALS and the spherical approximation for the free volume holes. Apparently, their results agreed very well with the theoretical free volume fractions; however, they introduced an ad hoc occupied volume that does not correspond to the one provided by the theory. Therefore, our first aim was to investigate the free volume fraction in IR without constraining the occupied volume to values in contrast with the theory. To this purpose, we guessed that non-spherical shapes for the free volume holes could restore agreement between the free volume fraction predicted from the theory and the one obtained from the experiment. Furthermore, we also aimed at obtaining some insight on the sizes needed to allow the mobility of the chains in the elastomeric state, that is, above the T_g. FKM was chosen in order to have a second rubber with a linear backbone, but with a saturated chain (IR has an unsaturated carbon chain) and different lateral groups ($-CF_3$ instead of $-CH_3$). This implies very different chemical–physical features (e.g., the glass transition in FKM occurs at much higher temperature than in IR, and the density is about twice that of IR). We aimed at ascertaining whether two elastomers, macroscopically different, behave differently also at microscopic level or, whether, on the contrary, they show analogies in the free volume structure.

Each linear molecule between two knots and above T_g can be regarded as a Gaussian chain when its length is sufficiently long in comparison with the Kuhn length, l_k.[18] Either in the melted state or in a theta-solvent solution, its average conformation is described as a random walk. As shown by Wang,[19] the effective bond length l_{eff}, defined as the square root of the ratio between the unperturbed mean-square end-to-end distance $\langle R^2 \rangle_0$ of a chain and the number of its backbone bonds, is rather constant. This implies that all of these polymers show comparable Kuhn lengths, such as

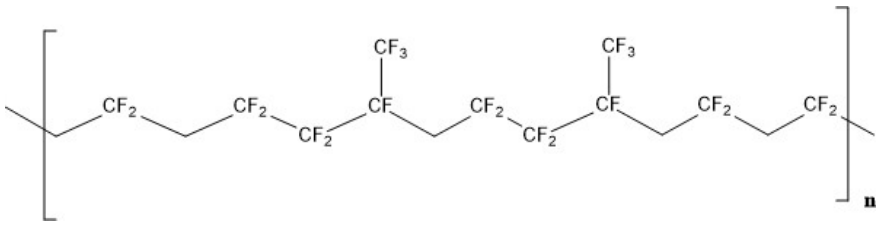

FIG. 1. — FKM polymer with a repeating unit $-[C_{16}H_{10}F_{22}]_n-$.

$$l_k = 3l_{\text{eff}} \approx 0.9 - 2\text{nm} \tag{2}$$

It is reasonable to assume that between physical knots, either entanglements or cross-links, the Kuhn segment contains about the same number of monomeric units (and therefore $l_{\text{eff}} = 0.5 \pm 0.2$ nm). Therefore, another goal of the present paper was to enlighten a possible correlation between size of the free volume hole and l_{eff}, in spite of the plausible different cross-link density of the two investigated elastomers. Again, the comparison between different elastomers could produce interesting results.

MATERIALS AND METHODS

MATERIALS

High *cis*-polyisoprene rubber (hereafter IR) from Kraton Corporation (commercial name: Cariflex IR03130; Kraton Corp., Houston, TX, USA) had a content of *cis*-1,4 polyisoprene >90%. The fluoro rubber (hereafter FKM and shown in Figure 1) was supplied by Solexis (compound name: Tecnoflon DP5900, fluorine content between 67 and 70%; Solexis, West Deptford, NJ, USA). They were used to prepare the cured samples tested in this paper. Both compounds have been mixed in a Banbury mixer for 4 min according with the recipes shown in Table I.

The peroxide used for both recipes is the 2,5-Bis(tert-butylperoxy)-2,5-dimethylhexane from Aldrich-Fluka (chemical name Luperox 101, technical grade 90%, CAS Number: 78-63-7; Aldrich-Fluka, St. Louis, MO, USA).

Compounds after 24 h at 296 K were molded by means of a compression hydraulic molding machine with a clamping force of 8×10^5 N to prepare a plaquette of cured material 20 cm × 20 cm × 2 mm. Both the compounds were tested by using a rubber process analyzer (RPA) from Alpha Technologies (Hudson, OH, USA), in accordance with ASTM D 5289, at 453 K for 15 min. Non-reversion was detected in the curing curves for both the compounds. Looking at the curing curves of RPA (not reported here), both compounds already show a degree of curing >0.9 after 8 min at 453

TABLE I
RECIPES USED TO PREPARE THE TWO INVESTIGATED RUBBERS

IR compound	FKM compound	Phr
IR	FKM	100
Peroxide	Peroxide	1.5
	MgO	3
	Triallylisocyanurate (TAIC)	3

K. Therefore, they both have been cured in the press for 10 min to reach a fully cured state, by using the recipe described in Table I.

The curing conditions were followed by a postcuring thermal treatment in air ventilated oven as follows: (1) Compound IR: 1 h at 393 K. (2) Compound FKM: 10 h at 503 K.

The postcuring time and temperature were selected according to the recommendations of the rubber and fluoroelastomers producers in their technical reports of peroxide cured compounds, to improve the mechanical properties.[20]

All the subsequent analyses were carried out on the cured samples.

THERMAL ANALYSIS

Thermal analysis was performed using a Mettler-Toledo DSC 822e differential scanning calorimeter (Mettler-Toledo, Columbus, OH, USA), calibrated with high purity indium standard. Samples (between 5 and 10 mg) were encapsulated in aluminum pans and heated from 180 to 310 K at a rate of 10 K/min under nitrogen flux, to determine the glass transition temperature. This last was obtained as the inflection point of the heat capacity increment ΔC_p associated with the glass-to-elastomeric transition. It resulted in 214 $\pm$ 1 K and 271 $\pm$ 1 K for IR and FKM, respectively.

SPECIFIC VOLUME

Specific volume of cured samples of FKM and IR was initially determined at 298 K as the inverse of the density ρ. It was measured by means of a Sartorius balance (model ME215P: readability 10^{-5} g, repeatability 1.5×10^{-5} g; Sartorius, Göttingen, Germany), equipped with a kit for the measurement of the density. Water was used as fluid. It resulted in values of $\rho = 1.875 \pm 0.003$ g/cm^3 and 0.921 ± 0.002 g/cm^3 for FKM and IR, respectively.

PVT MEASUREMENTS

The experiments were performed with a commercial pressure volume temperature (PVT) confining fluid dilatometer (Gnomix Inc., Bloomington, IN, USA). For the dilatometry measurements, small samples having an approximate volume of 1 cm^3 were cut from the available rubber slabs. Mercury was employed as a confining fluid.

The PVT surface was explored through isothermal compressions from 10 to 200 MPa, measuring volume variation data each 5 MPa. A sequential protocol was adopted, starting at 303 K and increasing temperature by 10 K after the end of each isotherm compression stage. The explored temperature range was 303–373 K for IR and 303–443 K for FKM. The temperature intervals were chosen in order to avoid any possible degradation of the investigated compounds. Each protocol was performed twice on the same sample. Data measured at high pressure were extrapolated to 0.1 MPa through the application of the Tait equation.[8]

The measured relative variations of specific volume were converted to absolute specific volume, V, by requiring that the value extrapolated from the PVT experimental data to 298 K would coincide with that measured by buoyancy methods in the same conditions, as usual in these investigations.[8]

PALS

PALS measurements were performed using cylindrical samples (diameter: 2 cm), whose thickness (2 mm) granted that all the positrons entering in each of them were annihilated. The positron source, ^{22}Na embedded between two Kapton® foils (thickness about 7 μm each), was placed inside a copper cup containing the sample and in contact with the heat exchanger of a liquid

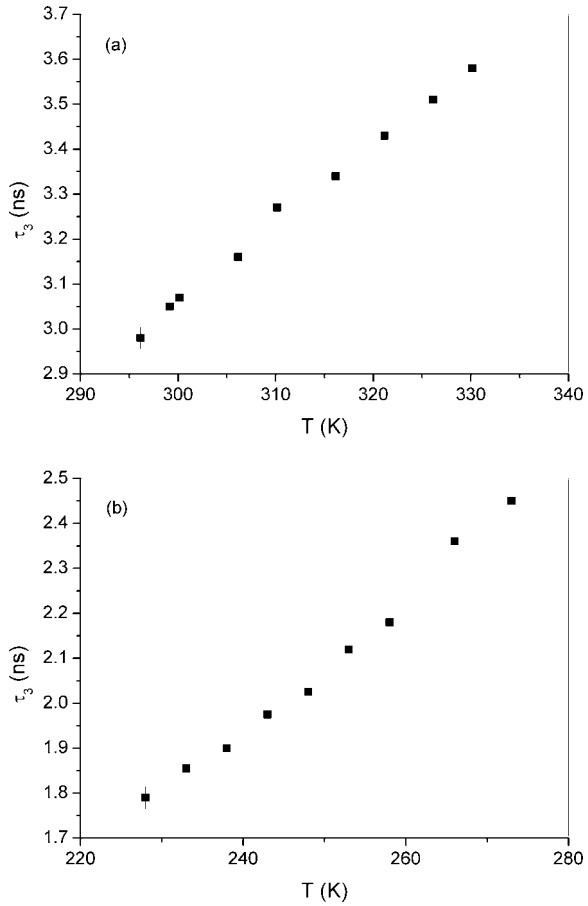

FIG. 2. — *o*-Ps lifetime τ_3 in FKM (a) and in IR (b) vs temperature. Typical experimental uncertainties (as derived from the scattering of the data) are shown for the data at the lowest temperature.

nitrogen cryostat (DN 1714 Oxford Instruments, Abingdon, UK). Temperature was stable within 0.5 K. The temperature ranges for the investigated elastomers are 296–330 K and 228–273 K for FKM and IR, respectively. The lowest temperature was chosen above the glass transition temperature in order to always keep the samples in equilibrium. Measurements were performed at a pressure $<10^{-5}$ mbar. A timing spectrometer with a resolution of about 270 ps collected the positron spectra (three spectra for each temperature). Each spectrum contained at least 2×10^6 counts and was analyzed by means of the *LT* program[21] with a proper correction for the positrons annihilated in the Kapton support.

RESULTS AND DISCUSSION

Positron annihilation lifetime spectra were deconvoluted in three components, obtaining a satisfactory statistical test (normalized χ^2 in the range 0.91–1.12). The shortest lifetime component (around 0.18 ns) comes from annihilation of positrons in the bulk as well as from *p*-Ps. The intermediate component (about 0.4 ns) is attributed to positrons annihilated in regions with lower electron density than the bulk (such as defects and free volume holes), which explains the longer lifetime compared with the shortest component. The longest component is due to *o*-Ps annihilated

inside the free volume holes. Behavior of *o*-Ps lifetime τ_3 versus the temperature in the two investigated compounds is displayed in Figure 2.

The investigated range of temperatures is above the glass transition for both the compounds, and the trend of τ_3 is linear with temperature (correlation coefficients are 0.998 and 0.994 for FKM and IR, respectively). At suitably high temperatures (around 300 K for IR and 340 K for FKM) the slope of $\tau_3(T)$ decreases; this feature, not reported in Figure 2, is commonly observed in many materials. It is probably due to a sufficiently short relaxation time of the molecular segments, which involves a decreased lifetime of the hole. When it becomes comparable to Ps lifetime,[22] it is no longer possible for Ps to correctly probe the size of the cavity.

The lifetime values of *o*-Ps have to be converted into mean sizes of the free volume holes. To this purpose a quantum mechanical model framing Ps in the cavity is needed. The most popular one is the Tao-Eldrup model:[9,10] the cavity is a spherical void with radius R. The potential well of the depth is infinite, and a thickness ΔR (=0.166 nm; refs 10, 23) is introduced to take into account the penetration of the Ps wave function into the bulk. The electron density is assumed constant for $r > R$ and zero for $r < R$. The model produces the following equation:

$$\lambda_p = \lambda_0 \left[\frac{\Delta R}{R + \Delta R} + \frac{1}{2\pi} \sin\left(2\pi \frac{R}{R + \Delta R} \right) \right] \tag{3}$$

where λ_p is the pickoff decay rate and $\lambda_0 \cong 2\ \mathrm{ns}^{-1}$ is the annihilation rate of *o*-Ps in the presence of a high electron density. The *o*-Ps lifetime τ_3 is the inverse of the total decay rate λ_3, sum of the pickoff decay rate and the intrinsic decay rate $\lambda_i = 1/142\ \mathrm{ns}^{-1}$:

$$\tau_3 = 1/\lambda_3 = 1/(\lambda_p + \lambda_i) \tag{4}$$

Assuming non-spherical geometries for the cavity model produces different relationships between pickoff decay rate and typical size of the hole.[24–27] If the spherical geometry is used, the hole volume obtained is $v_h = (4/3)\pi R^3$.

In order to evaluate the free volume, we need specific volume data; dilatometry results are therefore essential. They are displayed for the two rubbers in Figure 3, where a linear dependence of the specific volume V on the temperature is found (correlation coefficient >0.999). We used these data to find the number density of free volume holes (see below), but also to fit the Simha–Somcynsky equation of state,[12] valid for amorphous polymers at equilibrium.[13,28] This equation of state is represented at atmospheric pressure by the following pair of equations:

$$\tilde{T} = 2y(y\tilde{V})^{-2}\left\{1.2045 - 1.011(y\tilde{V})^{-2}\right\}\left\{1 - 2^{-1/6}y(y\tilde{V})^{-1/3}\right\} \tag{5a}$$

$$1 + y^{-1}\ln(1-y) = \left(\frac{y}{6\tilde{T}}\right)(y\tilde{V})^{-2}\left\{2.409 - 3.033(y\tilde{V})^{-2}\right\} + \left\{2^{-1/6}y(y\tilde{V})^{-1/3} - 1/3\right\}\left\{1 - 2^{-1/6}y(y\tilde{V})^{-1/3}\right\}^{-1} \tag{5b}$$

where reduced thermodynamic coordinates $\tilde{T} = T/T^*$ and $\tilde{V} = V/V^*$ appear. The scaling parameters T^* and V^* depend on the material and are found by fitting Eqs. 5a and 5b with the specific volume data. Alternatively, the following simpler polynomial expression[29] can be used:

$$\ln\left(\frac{V}{V^*}\right) = a + b\left(\frac{T}{T^*}\right)^{3/2} \tag{6}$$

The two procedures produce the same results, within the errors. For FKM we found $V^* = 0.5163 \pm 0.0003\ \mathrm{cm}^3\ \mathrm{g}^{-1}$ and $T^* = 9161 \pm 26$ K. Concerning IR, the result is: $V^* = 1.0535 \pm$

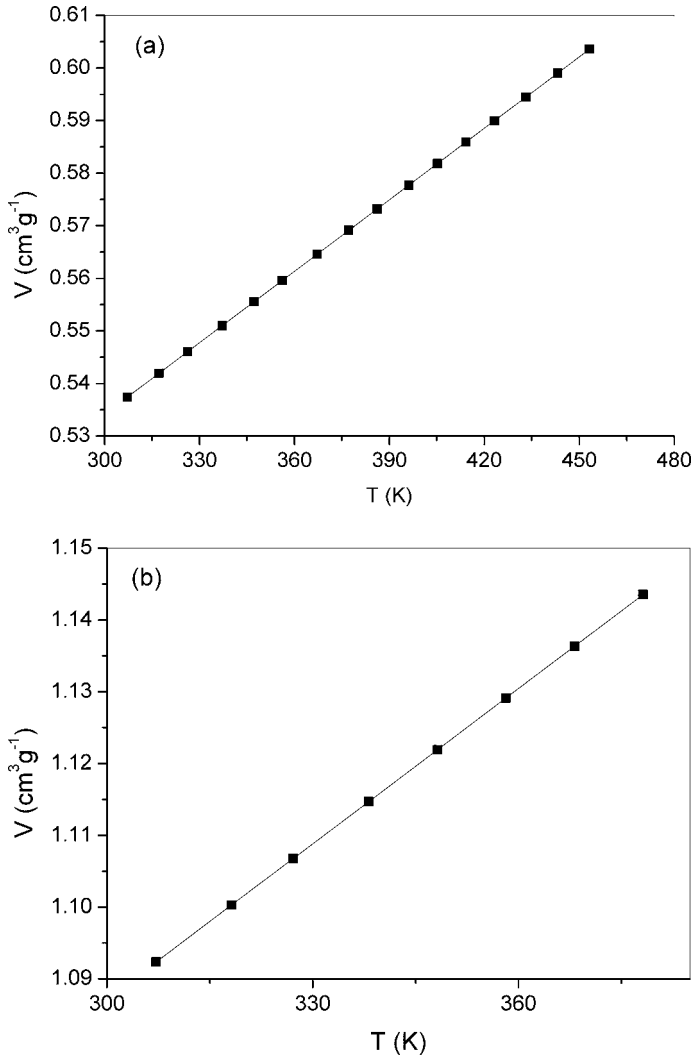

FIG. 3. — Specific volume V as a function of the temperature T in FKM (a) and IR (b). Experimental uncertainties (as derived from the scattering of the data) are within the symbols.

0.0004 cm^3/g; $T^* = 9547 \pm 29$ K. In Eq. 5, y represents the volume fraction of occupied sites, and $h = 1 - y$ is the calculated free volume fraction,[30] which is adapted to our rubbers once we know the scaling parameters.

According to the theory, y depends on the temperature; the thermal expansion coefficient is typically $<4\times10^{-5}\,K^{-1}$ for polymers.[31] In the present study we took this dependence of the specific occupied volume into account, V_{occ} on the temperature, although a constancy of V_{occ}, as generally adopted in the literature,[27,31] is already a good approximation, .

Since the specific volume V is the sum of the specific free volume and the specific occupied volume:

$$V = Nv_h + V_{occ} \tag{7}$$

it is possible to evaluate the fractional free volume f as

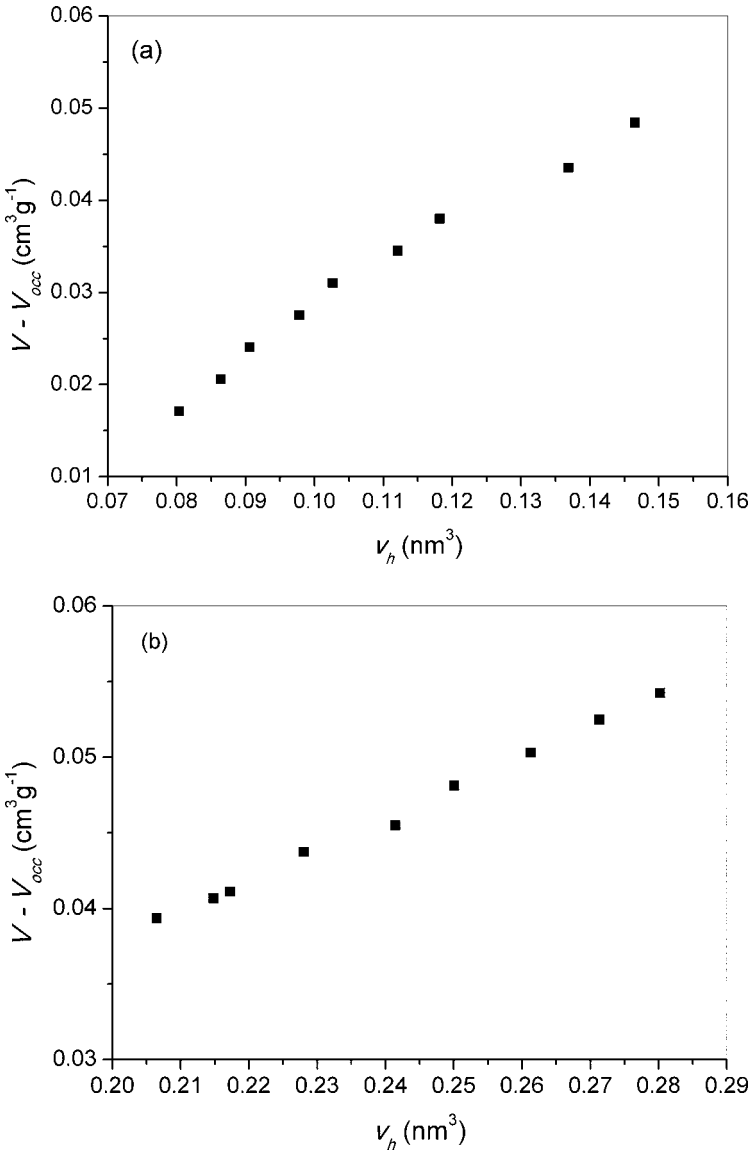

FIG. 4. — Specific free volume $V - V_{\mathrm{occ}}$ vs the hole volume v_h in FKM (a) and in IR (b), calculated using the spherical approximation.

$$f = \frac{V_f}{V} = \frac{N v_h}{N v_h + V_{\mathrm{occ}}} \tag{8}$$

PALS and dilatometric data allow us to find N through the fitting procedure shown in Figure 4, where the specific free volume $V - V_{\mathrm{occ}}$ is plotted versus v_h in the range of temperatures investigated by PALS.

For the analyzed structures, N can be assumed constant, that is, independent of the temperature, due to the linear dependence of $V - V_{\mathrm{occ}}$ on the average hole volume v_h, calculated using the Tao–

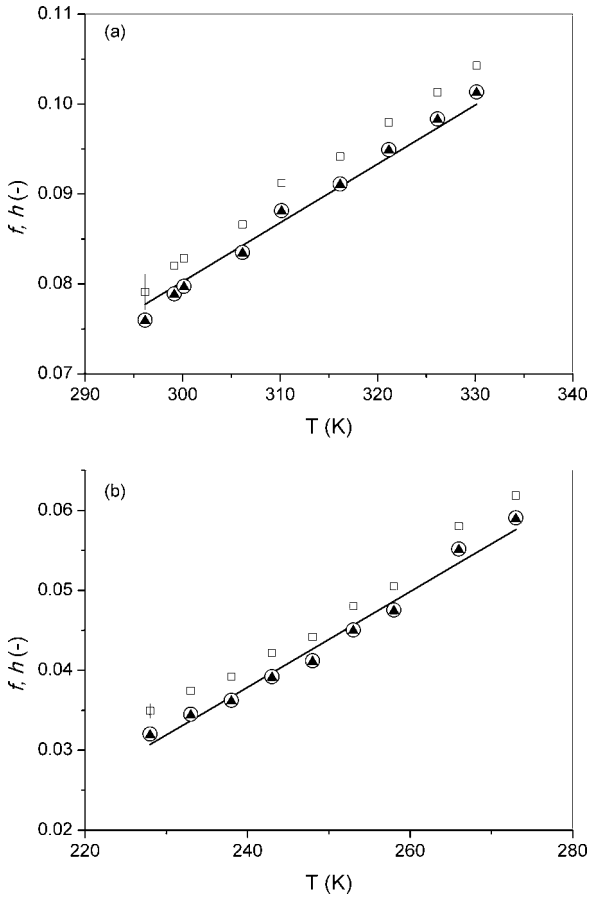

FIG. 5. — Free volume fraction *f* evaluated from PALS and dilatometry by approximating holes as spheres (empty squares), flattened cylinders (empty circles), or elongated cylinders (full triangles) for FKM (a) and IR (b). The continuous line is the free volume fraction *h*, as calculated from the lattice-hole model. Estimated uncertainties (as derived from the propagation of the errors) are shown for the data at the lowest temperature.

Eldrup equation (Eq. 3): the correlation coefficients are 0.998 for FKM and 0.991 for IR. A linear correlation is found also starting from non-spherical shapes for the holes; of course, the values of N are geometry dependent.

Often a linear relation between N and *o*-Ps intensity, I_3, is assumed, so that the free volume fraction f is written as

$$f = Cv_hI_3 \tag{9}$$

the constant C being dependent on the polymer structure. We deem that Eq. 9 should be cautiously considered. Indeed, it has been pointed out[32,33] that several factors other than the number density of holes contribute to Ps formation, and consequently to I_3. In particular, sequential PALS measurements of poly(methyl methacrylate) samples[33] over a wide range of temperatures showed that *o*-Ps intensity displays hysteresis; the effect has been attributed to processes of radiation chemistry in the terminal track of the positron, and in this case I_3 does not correctly reflect the variation in the number density of holes with temperature. For these reasons, we prefer to follow the alternative approach expressed in Eq. 8.

Once N is known, the free volume fraction f can be evaluated according to Eq. 8. Figure 5 shows the trend of f as a function of the temperature; the continuous line represents the theoretical free volume fraction h. It is evident that values of f obtained using a spherical cavity geometry (empty squares in Figure 5) are systematically higher than h.

We solved the discrepancy between f and h by means of a suitable choice for the shape of the free volume holes. The holes were approximated to finite cylinders with aspect ratio ξ between the height a and the radius R of the cylinder; to this purpose we used the following formula:[11,26]

$$\lambda_p = \lambda_0(1 - P_1P_2) \tag{10}$$

where

$$P_1 = \frac{a}{a + \Delta a} + \frac{1}{\pi} sen\left(\frac{\pi a}{a + \Delta a}\right) \tag{11}$$

$$P_2 = \frac{\int_0^{a_1 R/(R+\Delta R)} x J_0^2(x)dx}{\int_0^{a_1} x J_0^2(x)dx} \tag{12}$$

$J_0(x)$ is the Bessel function of the first kind of zero order, $a_1 = 2.4048$ is the first zero of $J_0(x)$, and λ_0 and ΔR (=Δa) have the same meaning as in Eq. 3. Previous formulas allow one to numerically obtain the radius R of the cylinder once the o-Ps lifetime is known. The hole volume becomes:

$$v_h = \pi R^2 a = \pi \xi R^3 \tag{13}$$

and depends on ξ, which is considered to be a free parameter. The variable v_h is calculated for all the investigated temperatures, for a given value of ξ and compared with the specific free volume $V - V_{occ}$, producing plots analogous to those shown in Figure 4 for spherical holes. The corresponding number density of holes, $N(\xi)$, is obtained, and the free volume fraction $f(\xi)$ is evaluated according to Eq. 8. The procedure is repeated by varying ξ until the best fit between $f(\xi)$ and the theoretical free volume fraction h is found.

A very good agreement between the theoretical and the experimental estimates of the free volume fraction was produced for $\xi = 2.4$ and 4 for FKM and IR, respectively (Figure 5, full triangles). Number density of holes N resulted in 2.1×10^{20} g^{-1} and 3.1×10^{20} g^{-1} for FKM and IR, respectively. Flattened ($\xi < 1$) cylinders cannot be excluded using only statistical considerations, since an acceptable fit is found also for values of ξ corresponding to 0.49 and 0.40 for FKM and IR, respectively (Figure 5, empty circles). Nevertheless, elongated cylinders ($\xi > 1$) are in compliance with the estimates supplied by molecular dynamics simulations. Indeed, computer simulations on macromolecules allow one to get the shape of the free volume holes. For instance, in poly(ethylene)-like macromolecules non-spherical shapes acquire importance when the size of the free volume hole increases.[34] Elongated holes were found in a simulation research of poly(vinyl methylether),[35] and similar shapes were considered in stiff chain polymers.[36]

Our findings do not depend on the particular shape chosen for the holes. Indeed, we also considered parallelepipeds with square base and ratio ψ between the height and the size of the base. The results were very similar to those obtained with cylinders (data not shown).

Lifetimes of o-Ps at 298 K in FKM and IR result in 3.02 and 2.78 ns, respectively. In the case of cylindrical elongated holes, this implies higher average volume for FKM (0.20 nm^3) than for IR (0.16 nm^3). On the other hand, the specific free volume V_f introduced in Eq. 1 (not to be confused with the free volume fraction f, Eq. 8) is higher for IR (0.050 cm^3 g^{-1}) than for FKM (0.042 cm^3 g^{-1}). This may

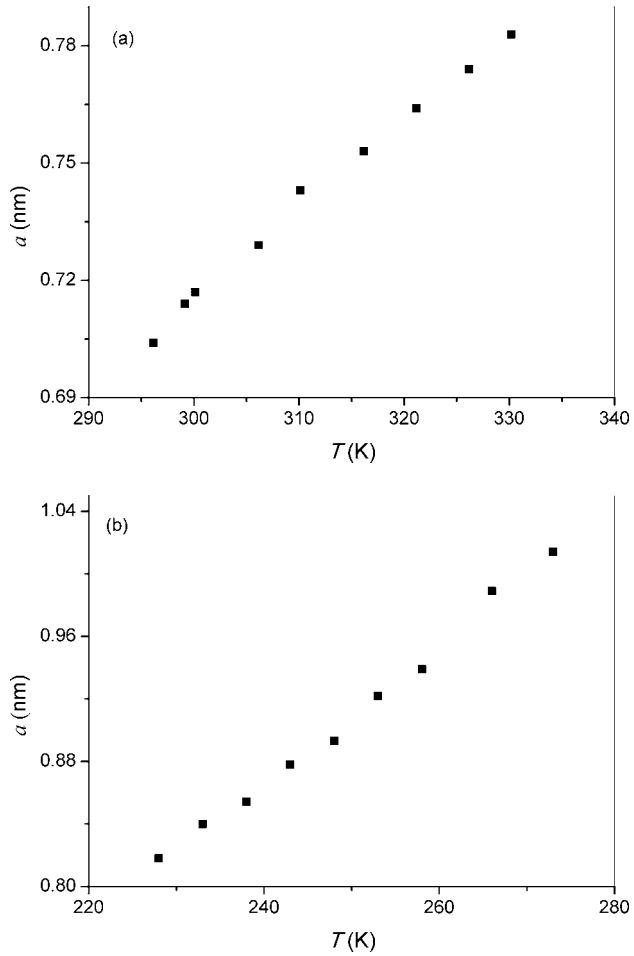

FIG. 6. — Behavior of the height a of the cylindrical elongated hole in FKM (a) and IR (b) vs temperature.

partially explain the higher air permeability of IR with respect to FKM at room temperature. On the other hand, the subject is complex, since the free volume is related to the diffusivity of a molecule throughout a membrane, while permeability depends on both the diffusivity and the solubility.

The guess of elongated, rather than flattened, cylindrical holes is interesting also for the following reason. From the previously described procedure, to get the cylindrical hole volume we can obtain the trend of the height $a = \xi R$ of the hole versus the temperature. The results, shown in Figure 6, point out a linear increase of a, which allows us to obtain, by extrapolation, the height of the cavity at the glass transition temperature, $a(T_g)$:

$$a = a(T_g)\left[1 + \beta(T - T_g)\right] \tag{14}$$

This last quantity is very similar to the two investigated compounds (0.65 and 0.75 nm for FKM and IR, respectively) and comparable to the effective bond length estimated by Wang,[19] equal to 0.5 $\pm$ 0.2 nm. Milner[37] reported the value 0.6 nm. This result is in agreement with the physical interpretation of the transition from the glassy to the elastomeric state and the resulting increased mobility in the chain segments due to the enhancement of the free volume.

CONCLUSIONS

A previous work[7] demonstrated the capability of PALS to reproduce, at least qualitatively, the behavior of the free volume fraction in IR versus the temperature, as estimated by the lattice-hole theory. Nevertheless, values of the occupied volume systematically higher than those provided by the theory had to be introduced, using the spherical approximation for the holes. In the present work, we showed that the issue can be solved by allowing the holes to assume a cylindrical shape. This is in agreement with results from computer simulations, which generally predict elongated, rather than spherical shapes. By comparing the free volume fraction f as estimated from dilatometry and PALS results with the theoretical predictions, we were able to deduce more precise values of f versus temperature. The procedure gave us some insight about the shape of the free volume holes; of course, information is approximate, since real holes are irregular. Note the role played by the specific volume measurements. In fact, they supply the thermodynamic parameters necessary to calculate the theoretical free volume fraction. Furthermore, they allow one to deduce the number density of holes in combination with PALS data and therefore to build a free volume fraction without reference to the *o*-Ps intensity, a controversial parameter due to its dependence on the chemistry of the material[32] and on irradiation effects.[33] Presently, on the basis of bare statistical reasoning, our results do not allow us to discriminate between elongated and flattened holes, but we can conclude that in the investigated rubbers a cylindrical geometry is a better approximation than the spherical one and allows a better representation of the free volume fraction. In order to get a better understanding of the hole morphology in rubbers, computer simulations of our elastomers would be needed, which are rather time consuming. Nevertheless, a clue in favor of elongated shapes comes from the comparison between the average height of the free volume cylindrical hole at T_g and the effective bond length, l_{eff}. Indeed, by assuming cylinders with aspect ratio $\xi > 1$, our results show that the two quantities are comparable. It is a reasonable result, taking into account the role played by the free volume in the mobility of the macromolecular chain.

REFERENCES

[1]O. E. Mogensen, *Positron Annihilation in Chemistry*, Springer, Berlin, 1995.

[2]J. J. Algers, F. H. J. Maurer, M. Eldrup, and J. S. Wang, *J. Mater. Sci.: Mater. Med*. **14**, 955 (2003).

[3]S. S. Jordan and W. J. Koros, *Macromolecules* **28**, 2228 (1995).

[4]J. D. Ferry, *Viscoelastic Properties of Polymers*, 3rd ed., John Wiley & Sons, New York, 1980.

[5]J. G. Victor and J. M. Torkelson, *Macromolecules* **20**, 2241 (1987).

[6]S. Berko and H. N. Pendleton, *Ann. Rev. Nucl. Part. Sci*. **30**, 543 (1980).

[7]R. Srithawatpong, Z. L. Peng, B. G. Olson, A. M. Jamieson, R. Simha, J. D. McGervey, T. R. Maier, A. E. Halasa, and H. Ishida, *J. Polym. Sci. Part B: Polym. Phys*. **37**, 2754 (1999).

[8]D. Walsh and P. Zoller, *Standard Pressure Volume Temperature Data for Polymers*, 1st ed., CRC Press, Boca Raton, FL, 1995.

[9]S. J. Tao, *J. Chem. Phys*. **56**, 5499 (1972).

[10]M. Eldrup, D. Lightbody, and N. J. Sherwood, *Chem. Phys*. **63**, 51 (1981).

[11]G. Consolati, *J. Chem. Phys*. **117**, 7279 (2002).

[12]R. Simha and T. Somcynsky, *Macromolecules* **2**, 342 (1969).

[13]P. A. Rodgers, *J. Appl. Polym. Sci*. **48**, 1061 (1993).

[14]J. Choi and A. I. Isayev, RUBBER CHEM. TECHNOL. **86**, 633 (2013).

[15]V. M. D. Pasa, A. V. Maciel, J. C. Machado, and G. O. Barra, RUBBER CHEM. TECHNOL. **85**, 195 (2012).

[16]K. S. Bandzierz, L. A. E. M. Reuvekamp, J. Dryzek, W. K. Dierkes, A. Blume, and B. M. Bielinsky, RUBBER CHEM. TECHNOL. **92**, 69 (2019).

[17]W. Salgueiro, A. Marzocca, A. Somoza, G. Consolati, S. Cerveny, F. Quasso, and S. Goyanes, *Polymer* **45**, 6037 (2004).

[18]L. J. Fetters, D. J. Lohse, and R. H. Colby, "Chain Dimensions and Entanglement Spacings," in *Physical Properties of Polymers Handbook*, 2nd ed. J. E. Mark, Ed., Springer, Berlin, 2005.

[19]S. Q. Wang, *Macromolecules* **40**, 8684 (2007).

[20]https://www.chemours.com/Viton/en_US/assets/downloads/viton-oven-post-curing-parts-technical-information.pdf

[21]J. Kansy, *Nucl. Instr. Methods Phys. Res., Sect A* **374**, 235 (1996).

[22]J. Bartoš, O. Šauša, D. Racko, J. Krištiak, and J. J. Fontanella, *J. Non-Cryst. Solids* **351**, 2599 (2005).

[23]H. Nakanishi, S. J. Wang, and Y. C. Jean, "Microscopic Surface Tension Studied by Positron Annihilation," in *Positron Annihilation Studies of Fluids*, S. C. Sharma, Ed., World Scientific, Singapore, 1988.

[24]B. Jasinska, A. E. Koziol, and T. Goworek, *J. Radioanal. Nucl. Chem*. **201**, 617 (1999).

[25]Y. C. Jean and H. Shi, *J. Non-Cryst. Solids* **172**, 806 (1994).

[26]B. G. Olson, T. Prodpran, A. M. Jamieson, and S. Nazarenko, *Polymer* **43**, 6775 (2002).

[27]G. Consolati, F. Quasso, R. Simha, and B. G. Olson, *J. Polym. Sci., Part B: Polym. Phys*. **43**, 2225 (2005).

[28]L. A. Utracki, *J. Polym. Sci. Part B: Polym. Phys*. **42**, 2909 (2004).

[29]L. A. Utracki and R. Simha, *Macromol. Theory Simul*. **10**, 17 (2001).

[30]L. A. Utracki, R. Simha, and A. Garcia-Rejon, *Macromolecules* **36**, 2114 (2003).

[31]R. Simha and P. S. Wilson, *Macromolecules* **6**, 908 (1973).

[32]V. P. Shantarovich, *J. Radioanal. Nucl. Chem*. **210**, 357 (1996).

[33]C. L. Wang, T. Hirade, F. J. H. Maurer, M. Eldrup, and N. J. Pedersen, *J. Chem. Phys*. **108**, 4654 (1998).

[34]H. Don and K. I. Jacob, *Macromolecules* **36**, 8881 (2003).

[35]D. Račko, S. Capponi, F. Alvarez, J. Colmenero, and J. Bartoš, *J. Chem. Phys*. **131**, 064903 (2009).

[36]D. Hofmann, M. Entrialgo-Castano, A. Lerbret, M. Heuchel, and Y. Yampolskii, *Macromolecules* **36**, 8528 (2003).

[37]S. T. Milner, *Macromolecules* **38**, 4929 (2005).

[*Received February 2019, Revised July 2019*]